



flepiMoP: The evolution of a flexible infectious disease modeling pipeline during the COVID-19 pandemic

Joseph C. Lemaitre^{a,*}, Sara L. Loo^b, Joshua Kaminsky^c, Elizabeth C. Lee^c, Clifton McKee^c, Claire Smith^c, Sung-mok Jung^d, Koji Sato^b, Erica Carcelen^b, Alison Hill^e, Justin Lessler^{a,c,d,1}, Shaun Truelove^{b,c,1}

^a Department of Epidemiology, Gillings School of Global Public Health, University of North Carolina at Chapel Hill, Chapel Hill, NC, USA

^b Johns Hopkins University International Vaccine Access Center, Department of International Health, Baltimore, MD, USA

^c Department of Epidemiology, Johns Hopkins Bloomberg School of Public Health, Baltimore, MD, USA

^d Carolina Population Center, University of North Carolina at Chapel Hill, Chapel Hill, NC, USA

^e Institute for Computational Medicine, Johns Hopkins University, Baltimore, MD, USA

ARTICLE INFO

Keywords:

COVID-19
Influenza
Respiratory syncytial virus
Compartmental model
Forecasting
Scenario Planning
Pipeline
Open-source Software

ABSTRACT

The COVID-19 pandemic led to an unprecedented demand for projections of disease burden and healthcare utilization under scenarios ranging from unmitigated spread to strict social distancing policies. In response, members of the Johns Hopkins Infectious Disease Dynamics Group developed *flepiMoP* (formerly called the *COVID Scenario Modeling Pipeline*), a comprehensive open-source software pipeline designed for creating and simulating compartmental models of infectious disease transmission and inferring parameters through these models. The framework has been used extensively to produce short-term forecasts and longer-term scenario projections of COVID-19 at the state and county level in the US, for COVID-19 in other countries at various geographic scales, and more recently for seasonal influenza. In this paper, we highlight how the *flepiMoP* has evolved throughout the COVID-19 pandemic to address changing epidemiological dynamics, new interventions, and shifts in policy-relevant model outputs. As the framework has reached a mature state, we provide a detailed overview of *flepiMoP*'s key features and remaining limitations, thereby distributing *flepiMoP* and its documentation as a flexible and powerful tool for researchers and public health professionals to rapidly build and deploy large-scale complex infectious disease models for any pathogen and demographic setup.

1. Introduction

From the emergence of SARS-CoV-2 in 2019 through the declaration of the global pandemic in March 2020 and the current landscape towards endemicity, it has been critical for decision-makers to be empowered with epidemiological models for better-informed decision-making. A large effort was enlisted to forecast and project the spread of the virus, and to investigate the effect of public health interventions on health outcomes. It is within this context that the “FLEXible EPIdemic MOdeling Pipeline” (*flepiMoP*; formerly known as the COVID Scenario Modeling Pipeline or CSP) was built. While many software pipelines were created or adapted for use during the pandemic, most were designed specifically around a single model structure (Bouchnita et al., 2024) or a specific spatial setup (Pillai et al., 2024; Rosenstrom et al., 2024).

2024). However, other flexible frameworks were developed, characterized by their scale of representation: from agent-based modeling frameworks, such as GLEaMviz/LEAM-US, FRED, EpiHiper, EpoSimS, CovaSim, EMOD (Bershteyn et al., 2018; Broeck et al., 2011; Chen et al., 2024; Chinazzi et al., 2024; Kerr et al., 2021; Mniszewski et al., 2008; Moore et al., 2024), to compartmental metapopulation models such as *flepiMoP*, UVA-adaptive (Porebski et al., 2024) and SIKJALPHA (Srivastava, 2023; Srivastava et al., 2020), also including more general statistical modeling packages such as *pomp* (Asfaw et al., 2023; King et al., 2015).

In this diverse landscape, *FlepiMoP* stands out as a versatile and actively developed open-source software suite for simulating a wide range of compartmental models of infectious disease transmission. The disease transmission and observation models are defined by a no-code

* Corresponding author.

E-mail address: jo.lemaitresamra@gmail.com (J.C. Lemaitre).

¹ Denotes equal contribution

configuration file, allowing a breadth of models to be specified consistently, from simple SIR-style models in a single population to more complex models of multiple pathogen strains transmitting between thousands of connected metapopulations and age groups. In the context of the [COVID-19 Scenario Modeling Hub](#) (SMH, [COVID-19 Scenario Modeling Hub](#), 2020; Loo et al., 2024) and the [COVID-19 Forecast Hub](#) (FCH, [COVID-19 Forecast Hub](#), 2020; Cramer et al., 2022a), *flepiMoP* is used to model transmission of SARS-CoV-2 in the US at the state level using a compartmental metapopulation structure. The fifty US states are connected through human mobility and most epidemiological processes (e.g., vaccinations, the emergence of variants, waning immunity) are simulated mechanistically.

The main features of *flepiMoP* are:

- Open-source (GPL v3.0) infectious dynamics modeling software, written in R and Python;
- Versatile, no-code design that can be applied to compartmental and outcome observation models, allowing for quick application to epidemic events (e.g., emergence of new variants, vaccines, non-pharmaceutical interventions (NPIs));
- Powerful, just-in-time compiled disease transmission model and distributed inference engine ready for large-scale simulations on high-performance computing clusters or cloud workflows;
- Adapted to small- and large-scale problems, from a simple SIR model to a complex model structure with hundreds of compartments on thousands of connected populations;
- Strong emphasis on mechanistic processes, with a design aimed at leveraging domain knowledge in conjunction with statistical inference;
- Portable for Windows WSL, MacOS, and Linux with the provided Docker image and an Anaconda environment.

The objective of this paper is to describe the evolution of *flepiMoP* through the COVID-19 pandemic and provide an overview of the pipeline. The first section details the changes introduced in response to both the changing pandemic and the corresponding shifting demands from decision-makers. The second section provides a detailed overview of the *flepiMoP* framework, its primary features, current capabilities, and limitations. This overview is built around an example use-case, detailing a model of the first two years of COVID-19 transmission in the US. We provide a glimpse of model outputs in the last section.

2. The evolution of *flepiMoP* throughout the COVID-19 pandemic

Formerly called *The Johns Hopkins COVID-19 Scenario Modeling Pipeline* (CSP), the development of *flepiMoP* started on February 28, 2020, to provide the California Department of Public Health (CDPH) with scenario projections for the spread of SARS-CoV-2 in the state at the county level and the expected impact on the healthcare system. In its initial form, *flepiMoP* consisted of four independent modules: i) an epidemic seeding and importation module, ii) a compartmental module for disease transmission simulation, iii) an observation model for the computation of health outcomes, and iv) a report generation module aimed at decision-makers (Lemaitre et al., 2021). This structure was sufficient at the initial stages of the pandemic and *flepiMoP* models successfully captured early epidemiological dynamics and uncertainties, allowing the production of reports tailored to inform various governmental entities (e.g., CDPH, US Centers for Disease Control and Prevention (CDC), FEMA).

flepiMoP has since been continuously evolving to address changes in the pandemic's complexity and to improve our ability to inform the public health response to infectious disease epidemics (Fig. 1). As months of epidemiological data became available, the first major change was the development of a fifth module for the inference of model parameters from data. This inference module consists of a Markov Chain Monte Carlo (MCMC) algorithm tailored to large-scale infectious disease modeling problems across connected subpopulations. It leverages massively parallel computing with many short chains to handle time-consuming epidemic simulations and high-dimensional parameter spaces. This allows *flepiMoP* to estimate location-specific parameters and calibrate models to past data and then produce short-term forecasts. The submission of such forecasts to the COVID-19 Forecast Hub began on April 28, 2020 (performance evaluated in Cramer et al., 2022b).

In December 2020, the response to the pandemic switched focus from NPIs to vaccination. This change prompted a rewrite of the disease transmission model to allow for parallel paths of infection based on the vaccination status of the population. Since vaccine allocation was highly age-dependent, the model was also expanded to explicitly track separate age groups (as opposed to using age-distribution-adjusted rates). The emergence of new SARS-CoV-2 variants with altered transmissibility and severity (e.g., Alpha in February 2021 and Delta in June 2021 (Davies et al., 2021; Taylor, 2021)), evidence for waning immunity, and evidence for the substantial immune escape of the Omicron variant

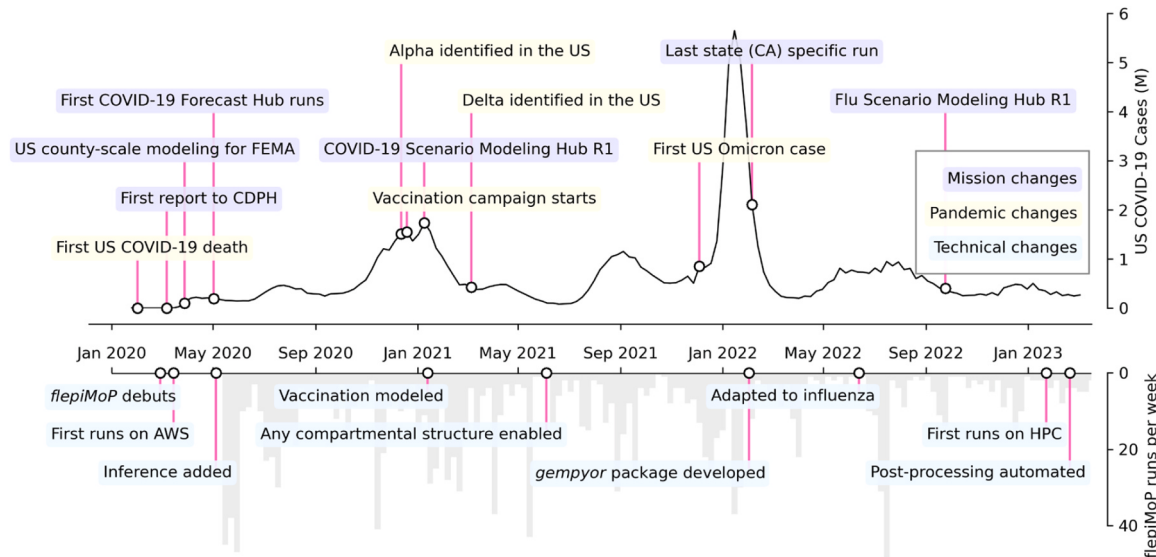


Fig. 1. The evolution of *flepiMoP* over the course of the COVID-19 pandemic. Timeline of COVID-19 cases reported in the US (in millions), with mission changes (purple) and epidemiological changes (yellow) highlighted. These changes directed the development of *flepiMoP* technical features (blue) while continuous modeling runs (gray bars) informed public health departments and the different multi-modeling hubs.

(Pulliam et al., 2022) further led to an extensive rewrite of the transmission module. The formerly hardcoded SEIR model is now a meta-population transmission module that can be adapted to most compartmental structures, including complex models of immunity and clinical progression, as well as stratification by age, multiple pathogen strains, or vaccination statuses. The transition rates between compartments can also vary across space and time. We also extended the observation model to allow for arbitrary decision trees and probabilities, delays, and duration changes in space and time. This extension allows *flepiMoP* to compute different health outcomes by age group, variant, or other strata and to represent features of the local health systems.

These changes allowed *flepiMoP* to adapt to the increasingly complex dynamics of the COVID-19 pandemic. However, changes also introduced increased computational complexity such that inference runs could take several days and generate hundreds of gigabytes of output data. To mitigate this, we refined a workflow that enables high-frequency, large-scale runs and rapid updates to the mechanistic model in a reproducible and computationally tractable way. To further manage the rapid changes and other new applications, we have developed a range of helper features, including a *config-writer* R package to quickly translate complex model requirements into the configuration file notation and post-processing tools to summarize the results and analyze model fits.

After three years of development and over 1500 model runs at varying scales, the *flepiMoP* software framework has reached a mature state with a stable feature set. The framework is capable of generating forecasts and scenario projections for most compartmental models of disease transmission at any geographical scale, with simultaneous calibration to multiple empirical data types. Notably, *flepiMoP* has been used to produce scenario projections of COVID-19 for the US COVID-19 Scenario Modeling Hub and various other locations, including Switzerland at the canton level, California at the county level, and South

Korea at the national level. The framework has also been successfully adapted for influenza forecasting and scenario projections for the CDC's FluSight (CDC, 2023) and the US Flu Scenario Modeling Hub with only minor modifications to the configuration files (Reich et al., 2019). These successes demonstrate *flepiMoP*'s versatility and effectiveness as a tool for modeling infectious diseases. *flepiMoP* is now available as an accessible tool for users who want to generate forecasts or scenario projections from a compartmental model at any scale, with in-depth documentation, vignettes, and template model setups available to all levels of users (flepiMoP.org).

3. *flepiMoP*: a flexible epidemic modeling pipeline

flepiMoP is divided into multiple composable submodules, as shown in Fig. 2. A single YAML configuration file defines the inclusion and behavior of each submodule over the specified population structure. The core module, *gempyor* ("General Epidemics Modeling Pipeline with Interventions and Outcome Reporting"), is a fast and flexible disease transmission model that can simulate any compartmental structure and observation model. *gempyor* can be run standalone for projection scenarios (given a set of parameters and without inference) or within a tailored, distributed *inference* module that executes several parallel chains of repeated epidemic simulations in an MCMC-like fashion, allowing for calibration of the model to data and identification of model parameters. As inference and simulation of large-scale problems are computationally costly, *flepiMoP* is provided with batch submission scripts for Slurm computing clusters or Amazon Web Service Batch. Around these modules, *flepiMoP* provides a toolbox of helper scripts to process data, store and retrieve model outputs, write configs, diagnose errors, and visualize results.

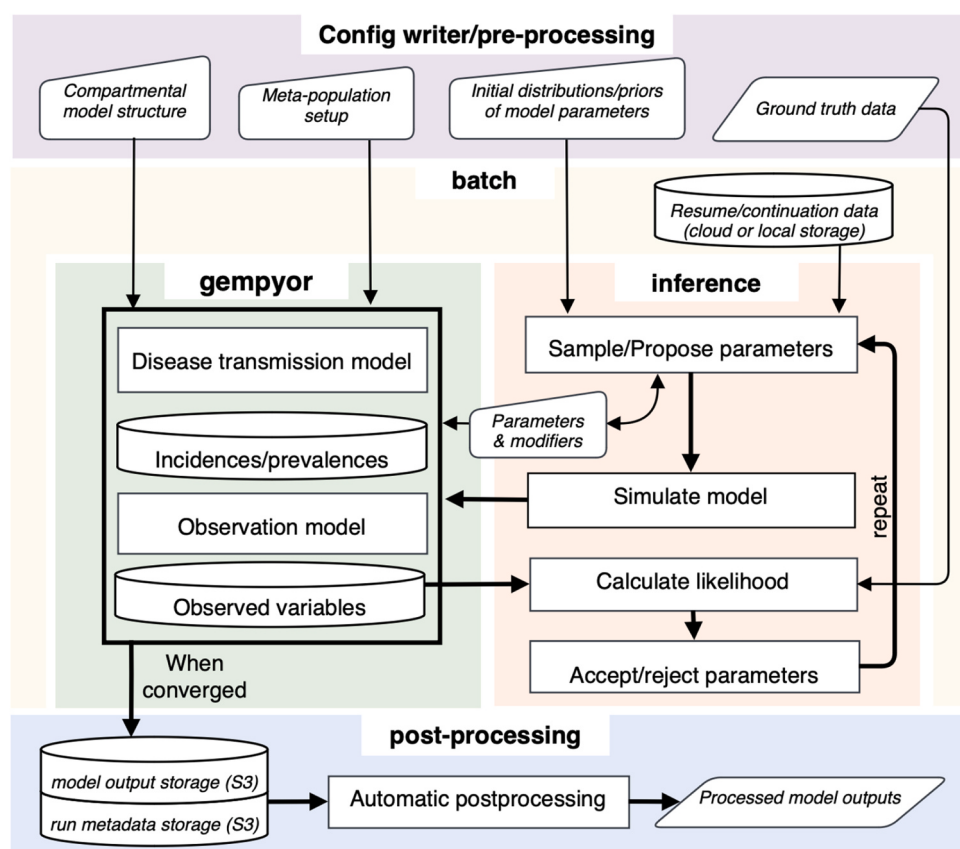


Fig. 2. Overview of the *flepiMoP* modules and their interactions during an inference run. Here we use standard flowchart symbols to represent the components of the pipeline and processes.

3.1. Population structure

flepiMoP operates over a defined demographic setup, with a single population or several connected subpopulations. The model inputs and outputs are specified for each population/subpopulation, and subpopulations can be connected by a mixing matrix.

For the US Scenario Modeling Hubs, we model the transmission of SARS-CoV-2 and influenza and their outcomes at the state level with fifty-one subpopulations, one for each US state plus the District of Columbia, connected through human mobility as measured by daily recurring commutes reported by the [US Census Bureau \(2015\)](#). Note that we have chosen to represent geographical locations as subpopulations and age classes as meta-compartments (see below). This is a convenient choice for generating state-level outputs aggregated across ages. However, one could represent both age structure and administrative units as subpopulations with no impact on the results.

4. Modeling infectious disease dynamics with *gempyor*

gempyor is an open-source Python package that constructs and simulates compartmental infectious disease dynamics models. *gempyor* is built to be used within *flepiMoP*, where it integrates with parameter inference and data processing scripts, but can also be run standalone with a command-line interface, generating simulations of disease incidence under different scenario assumptions.

4.1. Compartmental structure

The compartmental structure is defined as the product of so-called *meta-compartments*. For the example described below, the model featured 336 compartments in each of the 50 US states plus the District of Columbia, built from all possible combinations of the meta-compartments described in [Table 1](#).

Note that we model the infectious stage in three equivalent, chained compartments (with equal transition rates between compartments), which results in a Gamma-distributed residence time in the infectious compartment ([Champredon et al., 2018](#); [Cox, 2017](#); [Hurtado and Kirosingh, 2019](#)), a necessary modification to give realistically distributed serial intervals ([Galmiche et al., 2023](#); [Lloyd, 2001](#); [Wearing et al., 2005](#)). Moreover, we consider the waning of both vaccine-induced immunity and infection-induced immunity: an individual might have both waned levels of vaccine- and infection-induced immunity, full protection from both, or have only one source of immunity protection that has waned. This structure puts a strong emphasis on mechanistic dynamics and most transition rate parameters can be informed by the scientific literature.

Table 1

The compartmental structure of a *flepiMoP* model is constructed from meta-compartments and compartments. These model compartments were used to model the first two years of COVID-19 transmission in the US, from January 1st, 2020 to March 26, 2022.

Meta-compartments	Compartments
(7) Infection stages	Susceptible, Exposed, Infectious (divided into 3 subcompartments to approximate Gamma-distributed residence time), Recovered (with natural immunity), Waned (from natural immunity)
(4) Vaccination stages	Unvaccinated, vaccinated with 1 dose, with 2 doses, vaccinated with 1 or 2 doses but with waned vaccine-induced immunity
(4) Variant types	Wild type, Alpha, Delta, Omicron
(3) Age classes	Age 0–17, age 18–64, age 65–100 years

4.2. Transition rates between compartments

A transition between a source compartment X and a destination compartment Y in a subpopulation i is characterized by its rate, denoted $r_{X_i(t) \rightarrow Y_i(t)}(t)$ that is derived from user-provided (potentially time-varying, location-specific) parameters.

For most transitions, the rate depends only on the source compartment's X population. This is typical for transitions that approximate changes in a state based solely on time (such as waning, recovery, or the transition from $E \rightarrow I$) and for transitions caused by external forcing (such as vaccination). In a subpopulation i , the rate of these transitions is written as

$$r_{X_i(t) \rightarrow Y_i(t)}(t) = b_i(t) \bullet X_i(t)^{a_i(t)}$$

where X_i , Y_i are time-dependent variables describing the number of individuals in each compartment in subpopulation i , $a_i(t)$ is a unitless scaling parameter and $b_i(t)$ is the rate parameter (units: day⁻¹) in subpopulation i . In most cases, we have $a_i(t) = 1 \forall \{i, t\}$.

For the force of infection, the transition rate is proportional to other compartments' values. For example, the transition from S to E (new infections) is written as a mass-action law that depends on the number of infectious individuals I . For generality, and as infectious individuals may be spread among several meta-compartments, *flepiMoP* allows each transition to be proportional to an arbitrary number of groups (l) of compartments (m) that are summed together. This allows the transition from compartment S to compartment E to depend on the infected individuals in each age group and vaccination status. The rate governing these transitions is written as:

$$r_{X_i(t) \rightarrow Y_i(t)}(t) = X_i(t)^{a_i(t)} \cdot \prod_l \left[\underbrace{\left(1 - p_a \frac{1}{N_i} \sum_j M_{i,j} \right)}_{\text{prop. stay in } i} \cdot \underbrace{b_i(t) \frac{(\sum_m Z_{l,m,i}(t))^{a_{l,i}(t)}}{N_i}}_{\text{force of infection in } i} \right] + \sum_j \left[\underbrace{p_a \frac{1}{N_i} M_{i,j}}_{\text{prop. mixed } i \rightarrow j} \cdot \underbrace{b_j(t) \frac{(\sum_m Z_{l,m,j}(t))^{a_{l,j}(t)}}{N_j}}_{\text{force of infection in } j} \right]$$

where N_i is the population of subpopulation i and the compartments $Z_{l,m,i}$ are time-dependent variables describing the number of individuals in each compartment that influence the transition from X_i to Y_i ; these variables $Z_{l,m,i}$ may be X_i , Y_i or any other variable. Each element $M_{i,j}$ of the mixing matrix represents the number of individuals mixed daily from subpopulation i to j . These mixed individuals from subpopulation i spend a fraction p_a of the day in subpopulation j ($p_a = 0.5$ by default) and subsequently get exposed to infectious individuals in j .

These transition formulas provided enough flexibility to define models to track the COVID-19 pandemic in the US and the dynamics of influenza during the 2022–23 season. However, in its current state, *gempyor* does not allow rates that involve other nonlinear functions of compartments or parameters. As described in *flepiMoP* documentation, *gempyor* uses a compact syntax centered around transition groups for ease of defining the transition rates. One does not have to write the same transition for every age group or vaccination state, but can write an overall transition and how it is altered by age or vaccination. Coupled with the meta-compartment definition, these syntaxes enable fast iteration of the mechanistic structure, where it is straightforward to add a novel variant, an additional vaccine dose, or a different waning structure to the configuration file.

4.2.1. Simulation of the disease transmission dynamics

The epidemic simulation starts from the specified initial conditions, and additional introductions (or importations) may be seeded in any compartments over the course of the simulation. These initial conditions

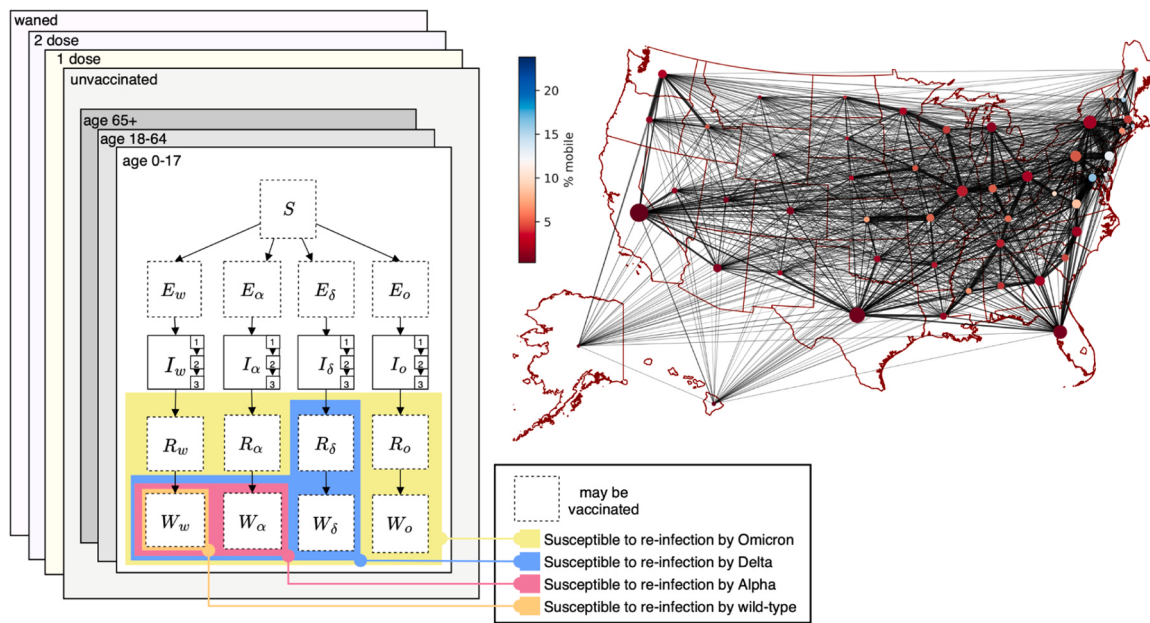


Fig. 3. Compartmental and population structure of an example *flepiMoP* model. The fifty US states' dynamics are coupled through human mobility, estimated here using US Census commuting data (edge width is the number of daily commuters between each state pair, the node size represents the state population, and the node color is the percent of individuals with interstate mobility). In each state, we model compartments for each variant, age category, and vaccination status. We highlight transitions between compartments for unvaccinated individuals less than 18 years old and indicate the possible transitions to other layers as dashed lines around compartments (possible vaccinations). Susceptible (S) can be exposed (E), and then infected (I) by different variants (w for wildtype, α for Alpha, δ for Delta, and o for Omicron), before waning a fraction of their immunity (W). The possible re-infections are color-coded to keep this diagram tractable.

and introductions are provided by the user or built by *flepiMoP*'s helper scripts.

The model can be simulated as a continuous-time, deterministic process, through a set of ordinary differential equations. For each transition between compartments X and Y , we have:

$$\begin{aligned} \frac{dX_i(t)}{dt} &= -r_{X_i(t) \rightarrow Y_i(t)}, \\ \frac{dY_i(t)}{dt} &= r_{X_i(t) \rightarrow Y_i(t)} \end{aligned}$$

gempyor proposes several methods to integrate these differential equations, including standard Python solvers. However, we have experienced that while accurate, these algorithms are too slow for large-scale epidemic simulations. To remedy this, we developed a modified, just-in-time compiled version of the Runge-Kutta 4 explicit integration scheme that delivers quick and accurate epidemic simulation at the timescale of most infectious disease dynamics problems. *gempyor* also provides lower-order explicit integration schemes, but we have experienced error buildup, leading to distorted predictions and misleading parameter estimation, even with small time steps.

Alternatively, the model can be treated as a continuous-time Markov Chain process, which we approximate as a discrete-time stochastic process using Euler-update-like binomial draws with exponential transition probabilities for computational practicability. The number of individuals transitioning between states X and Y between time t and $t + \Delta t$ is written as:

$$N_{X_i(t) \rightarrow Y_i(t)}(t) = \text{Binom}(X_i(t), 1 - e^{-\Delta t \frac{r_{X_i(t) \rightarrow Y_i(t)}}{X_i(t)}}),$$

$$N_{Y_i(t) \rightarrow X_i(t)} = -N_{X_i(t) \rightarrow Y_i(t)}(t)$$

Using stochastic or deterministic simulation, the disease transmission model produces daily incidence and prevalence in each compartment over the course of the simulation.

4.2.2. The observation model

In most real-life cases, the simulated incidence and prevalence are not directly observable. Within *gempyor*, it is possible to define an observation model that computes the observable quantities of interest from these variables. Typically, an observation model describes the process through which some subset of individuals from a source compartment is "observed", to compare simulations to ground truth data. For example, in the context of a model for an infectious disease like COVID-19, observable variables may include reported cases, hospitalizations, and deaths, but also virus concentration in wastewater or serostatuses.

The source of an observable variable is either a result of the epidemic model (e.g., the prevalence or the incidence in any set of compartments) or another already defined observable variable (e.g., intensive care patients drawn from hospitalized patients). Several pathways can lead to a single observable variable (e.g., pathways to death from infection can occur following hospitalization or from outside the healthcare system).

Mathematically, we generate an observable variable $H_i(t)$ from a source variable $X_i(t)$ as a transition defined by three time-varying parameters: a probability $p_i(t)$, its delay $q_i(t)$, and an optional duration $d_i(t)$. We draw individuals from the source with the given probability after the specified delay. For some outcomes, particularly those related to healthcare capacity (e.g., hospitalization, ICU occupancy), we also compute the prevalence in this outcome using the specified duration. For stochastic simulations, the incidence of the observable H in sub-population i is computed as:

$$\Delta H_i(t) = \text{Binom}(X_i(t - q_i(t)), p_i(t)).$$

Similarly, for deterministic simulations we compute:

$$\Delta H_i(t) = p_i(t) \cdot X_i(t - q_i(t)).$$

If a duration is specified, the prevalence of the observable is written as:

$$H_i(t) = \sum_{\tau=t-d_i(t)}^t \Delta H(\tau).$$

The main benefit of separating the computation of the observation process from the disease transmission simulation is the possibility of defining several observation models over the same (computationally costly) epidemic simulation scenario. Moreover, observable variables are defined with arbitrary delay and duration distributions, which naturally derive from observations of health-reporting practices instead of being limited to Erlang-distributed residential times in our mathematical modeling framework. At the time of writing, only point estimates of delay and duration are possible, and ongoing work is being conducted to enable functions that are then convolved, e.g., for representing a long-tailed hospitalization duration.

4.2.3. Parameters and modifiers

In the above description, we have used time-varying parameters to describe the observation model and the transition rates between compartments: the rates and exponent of the epidemic simulation model ($a_i(t)$, $b_i(t)$) and the probability, delay, and duration of the observation modules ($p_i(t)$, $q_i(t)$, $d_i(t)$). These parameters can be fitted and are defined by a fixed value, a distribution, or directly as a spatial time series. The latter is especially useful for assigning vaccination rates in each age group and US state or for covariates such as humidity, which can inform the seasonal force of infection for respiratory infections (Shaman et al., 2010).

The value of any parameter can be modified by multiplicative or additive modifiers. Each modifier applies to a parameter and changes its value in the specified (possibly discontinuous) time intervals and subpopulations. Several of these modifiers can apply simultaneously. In this case, their effect compounds, either additively, multiplicatively or multiplicatively as “reductions” depending on the user’s choice. In a subpopulation i , a parameter of value $p_i(t)$ affected by K modifiers $r_i^1(t), \dots, r_i^K(t)$ has a final value of:

$$p_i^*(t) = \begin{cases} p_i(t) + \sum_{k=1}^K r_i^k(t), & \text{with additive compounding} \\ p_i(t) \cdot \prod_{k=1}^K r_i^k(t), & \text{with multiplicative compounding} \\ p_i(t) \cdot \prod_{k=1}^K (1 - r_i^k(t)), & \text{with reduction compounding} \end{cases}$$

For the disease transmission model, we use these modifiers to alter the reproductive number to represent NPIs, seasonality, and local variation in transmission. For the observation model, modifiers may represent changes in case definition and changes in severity. It is possible to define several modifier scenarios within the same configuration file to project the impact under different NPIs or to reflect the uncertainty in an epidemiological feature. When ground truth data is available for observable variables, such as cases or deaths, both the underlying values of the parameters and their modifiers can be inferred by *flepiMoP*’s inference engine.

4.3. *flepiMoP* inference

flepiMoP proposes a custom Bayesian inference method inspired by Markov Chain Monte Carlo (MCMC) approaches and adapted to the particular challenges of large-scale epidemic models. Namely, MCMC chains with thousands of simulations take a long time, each model simulation taking several minutes, a duration that is prohibitive to the daily or weekly model runs that we require for rapid public health response. Instead, we exploit parallel computing resources by running a large number (typically 300) of short parallel chains, an approach that is becoming popular in parameter inference and has seen the development of suitable diagnostic criteria (Margossian et al., 2022). Moreover, we leverage the particular structure of the metapopulation compartmental model: in a spatial subpopulation, the dynamics depend more on the location-specific parameters than on the other locations’ dynamics. We

track two connected parameter chains with their own acceptance ratios:

- A *chimeric* (local) parameter chain that progresses independently in each region depending on the subpopulation-specific likelihood, and
- A *global* parameter chain that evolves based on the combined likelihood in all subpopulations.

When a parameter proposal is rejected at the global level, instead of being discarded, its location-specific components may be accepted individually in the chimeric chain.

Our inference algorithm is illustrated in Fig. 4. First, the proposed parameter set is drawn from a distribution that depends on the current chimeric parameters and we simulate the epidemic dynamics with *gempyor*. Then, the likelihood is computed at the global level, and a decision is made based on the ratio of the current parameter likelihood to the proposed parameter likelihood. If the proposed parameter is accepted, both chains are updated and there is no difference to classical MCMC. In the case of a rejection, we exploit the computation already done by accepting or rejecting each spatial subpopulation parameter set in the chimeric chain. As the subpopulations are only loosely connected, it is likely that the algorithm will help generate a better proposal for the next iteration.

We include two optional variations of our algorithm. The first, for loosely connected subpopulations, requires that the chimeric decision is made even in the case of global acceptance. In this case, a global acceptance does not overwrite the chimeric value. The second specifies a *chimeric-reset* frequency to prevent the chimeric chain from drifting too far from the global chain. After the chosen number of iterations, the chimeric chain is discarded and reset to the global chain. Note that if the *chimeric-reset* frequency is set to 1, the chimeric and global chain are equivalent and our inference engine acts as a classical MCMC scheme. In this case, all the theoretical convergence properties apply.

By default (when the *chimeric-reset* frequency is not set to 1), our method is not proven to converge towards the actual posterior distribution and offers no formal convergence guarantee for the short parallel chains we are using. However, we have reached a decent amount of empirical success – faster and more accurate calibration – compared to classical MCMC methods (Cramer et al., 2022b; Howerton et al., 2023). However, for use cases where theoretical convergence properties are necessary, we recommend the usage of the provided classical MCMC implementation (*chimeric-reset* frequency is set one) until we further develop the inference algorithm and our diagnostic tools.

In addition to *gempyor*’s parameters and modifiers, our inference algorithm is able to calibrate the number and the dates of foreign introductions (epidemic seeding) for each different SARS-CoV-2 variant over time. For the SMH, we inform most parameters from the literature (e.g., vaccine-induced protection against infection or death, age-dependent severity rate) in order to keep the parameter space to a reasonable dimensionality and improve identifiability. In the SMH Round 14, a total of 5720 parameters (not counting seeding), more than 100 parameters per US state, are fitted. This includes the infection-to-case ratio, the impact of NPIs, seasonality, and local variation in transmissibility. In the SMH Round 17 and in the example provided below, we fit our model to weekly-aggregated reported counts of hospitalizations for each US state from the U.S. Department of Health & Human Services (HHS), and deaths from the National Center for Health Statistics Mortality Surveillance System (reported in FluView) adjusted for variant prevalence estimates from [CoVariants.org](#) (Hodcroft, 2021).

5. Operational workflow

It is difficult to adapt a large-scale mechanistic model to rapidly changing epidemic dynamics and a shifting information landscape. *flepiMoP* proposes a comprehensive operational workflow in order to deliver up-to-date projections based on the latest available data. First, one may *resume* an inference run from a previous calibration.

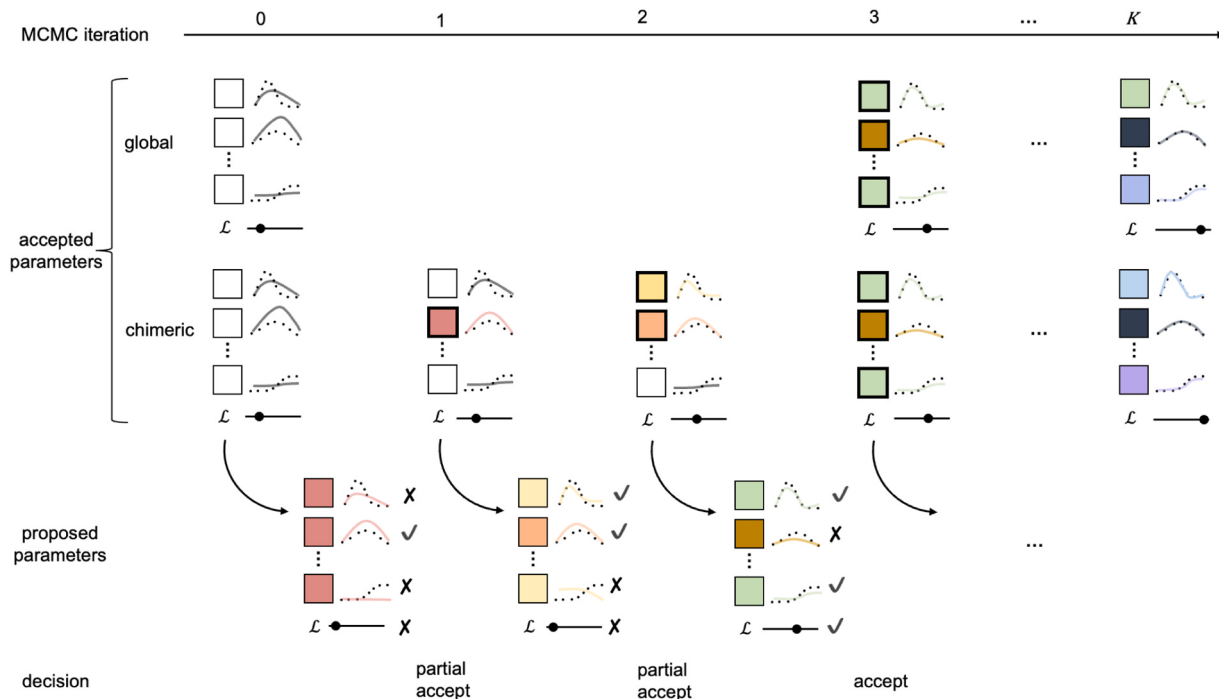


Fig. 4. Diagram of the custom multi-level MCMC method used for parameter inference in *fepiMoP*. This diagram represents a single MCMC chain, though multiple parallel chains are typically run and combined to form a posterior distribution of parameter values. Each square represents a single subpopulation that has a set of associated parameter values, and a dark black outline represents a partial acceptance from the previous iteration. The line at the bottom of each set of subpopulations represents the overall likelihood evaluation. Some parameters affect several (possibly all) subpopulations and are accepted on global acceptance).

Parameters that were already defined in a previous run are set to start at their last inferred values (fit during the previous run) while any newly introduced parameter is drawn from the initial distribution defined in the model configuration. Moreover, *fepiMoP* also allows one to *continue* a run from a previous run, taking as initial conditions the prevalence in every compartment for a certain date. For example, once satisfied with our fits from 2020–2022, we are able to run only the 2023 time period, if model assumptions are unchanged. Finally, we defined a precise bookkeeping and preservation workflow that is implemented in our batch submissions script for AWS Batch and Slurm HPCs. At every run, we store the model output along with metadata containing the exact *fepiMoP* and data versions, the key files to reproduce the run (e.g., the ground truth data), and a description of the run features (e.g., resume, continuation). Upon completion, the model output is uploaded to AWS S3 for future resumes and automatically post-processed for quick interpretation and analysis. These processed outputs are shared with the

modeling team on Slack with a provided bot, *fepiBot*.

As described in Fig. 5, we have extensively exploited these *continuation-resume* features as the landscape of variants, vaccinations, and NPIs has evolved throughout the COVID-19 pandemic response. We make regular updates to model structures, assumptions, and parameters. These updates are usually synced with rounds of the SMH and require longer calibration chains. In between, we provide weekly real-time forecasts (e.g., for submission to the FCH) with shorter calibration and small, compounding adjustments to the fit, with weekly updated epidemiological data. This approach has an added benefit as a rough approximation of a manual filtering algorithm: parameters are progressively defined as the data to characterize them becomes available, while other parameters are either already reasonably identified or not yet present. As such, the complexity of the mechanistic model formulation grows organically alongside the pandemic complexity, enabling only incremental updates of the epidemiologic assumptions and model

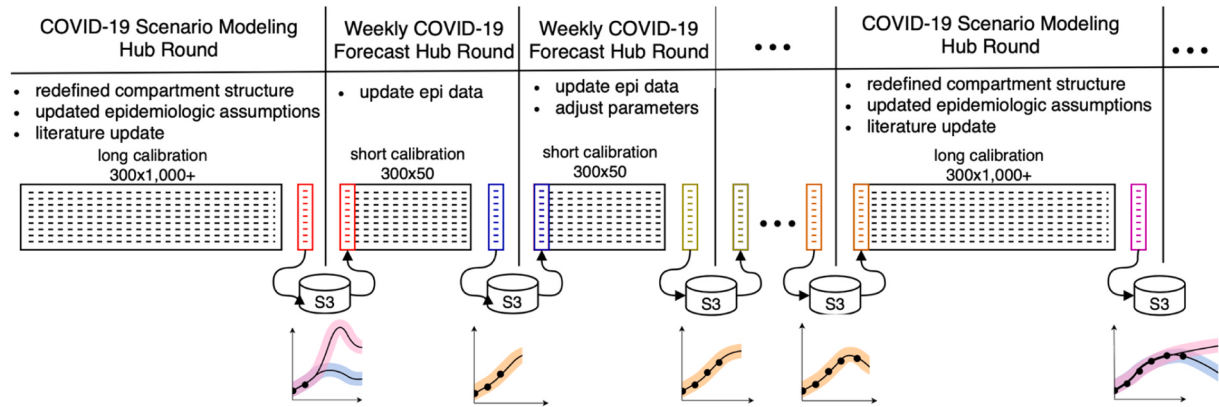


Fig. 5. : The operational workflow that allows *fepiMoP* to provide real-time projections of epidemics. The final value of our parallel chains is used as the initial conditions for latter fits. The size of the run is indicated as (number of parallel chains)x(number of iterations per chain).

and a distributed computational workload.

This operational workflow allows us to use the best available data and evidence to produce regular forecasts and projections of scenarios for decision-makers. We are able to take advantage of every single model evaluation and guarantee the reproducibility of our outputs while regularly updating the underlying model assumptions.

6. Showcase: modeling COVID-19 transmission in the US from January 2020 to June 2022

For this example, we used *flepiMoP* to model the first two years of COVID-19 transmission in the US, from January 1, 2020 to March 26, 2022. The compartments are described above in the table in the **Compartment structure** section. The global transmission rate parameter R_0 is modified at the state level by a variant-specific “local” transmission modifier and monthly seasonal modifiers, enabling calibrated shared inherent transmissibility with state-specific variability. The transmission rate is further modified within each state by parameters for the non-pharmaceutical interventions (phases of lockdown, reopening, and control measures in each state) defined from data we collected throughout the pandemic (built from data from the [Johns Hopkins University Coronavirus Resource Center](#), the [New York Times](#), and the [COVID Analysis and Mapping of Policies project](#)). The inferred state-specific variability and the NPI adjustments are shown in Fig. 6. Transmissibility and immunity are also modified by variants (Alpha, Delta, and Omicron), which are introduced into the model through seeding.

Age-specific vaccination is introduced from December 2020. Each successive dose is tracked and these have varied impacts on susceptibility through differences in vaccine effectiveness by variant. Immunity is further modified by cross-protection estimates based on variant, vaccination status, and waning, which is assumed to occur after a median of six months ([Goldberg et al., 2022](#); [Lumley et al., 2021](#)). The observation model computes the cases, hospitalizations, and deaths for each age group and variant (i.e., these rates are age-group and

variant-specific, and time-varying to match changes in case definitions and reporting procedures).

Finally, the inference is performed simultaneously on the weekly incident (non-variant) death and variant-specific hospitalization counts for each location with ground truth data from HHS and FluView, respectively. Due to the construction of this model and the defined “interventions” and periods we fit throughout, we are able to explicitly characterize the effects of each and the overall changing transmission within each location. The heterogeneity in transmission rate across states and over the duration of the pandemic can be seen in Fig. 6. This is based on seasonally adjusted variation between states (shown in blue in Fig. 6), as well as due to differences in implementation of NPIs in different states (shown in yellow in Fig. 6).

We also present our model fits for an example state (Massachusetts) in Fig. 7. We show the overall fit of multiple chains (Fig. 7A), as well as the variant-specific individual trajectories of each chain (Fig. 7B) for model outcomes showing infections, cases, hospitalizations, and deaths. Note that, as above, we only perform inference on hospitalization and death data.

7. Conclusions

After three years of continuous usage and over 1500 inference runs, *flepiMoP* is now entering a mature stage with a stable feature set, and we are releasing it along with comprehensive documentation. This modeling framework is aimed at enabling researchers and public health professionals to quickly build complex, large-scale mechanistic models of infectious disease transmission. As was experienced during the COVID-19 pandemic, and is now being seen with influenza and RSV, models like *flepiMoP* can provide highly valuable insights for evidence-based decision-making during both epidemic and endemic periods ([Borcherding et al., 2023](#)). The most important feature of *flepiMoP* is its flexibility to adapt to most epidemiological events through only a modified configuration file and input data, without requiring changes to the core model or other features. This adaptability has been successfully

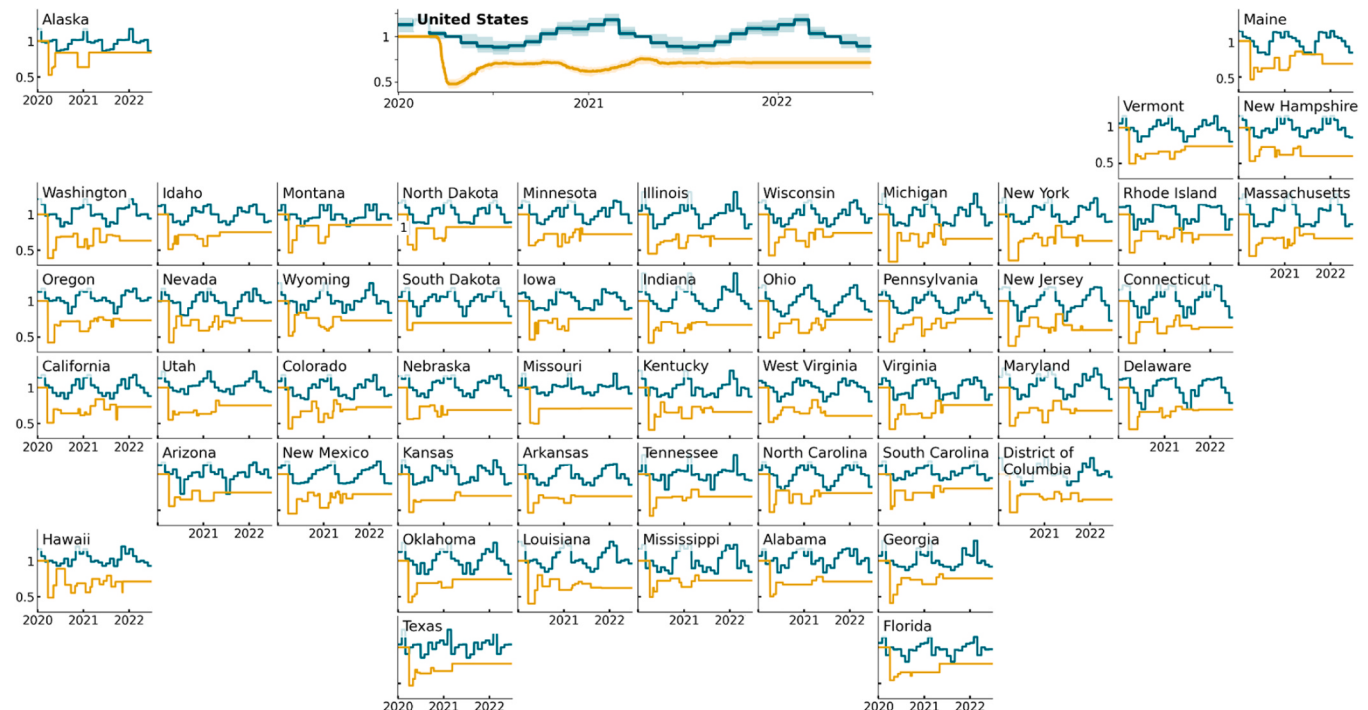


Fig. 6. Modifiers of the COVID-19 transmission rate inferred by *flepiMoP* from January 1, 2020 to March 26, 2022. We derive the spatiotemporal heterogeneity of our projections from the effect of the NPI (yellow line: median inferred value for each state, while the US mean is shown with the 50% and 95% confidence interval) and the seasonality adjusted with local variance (blue line).

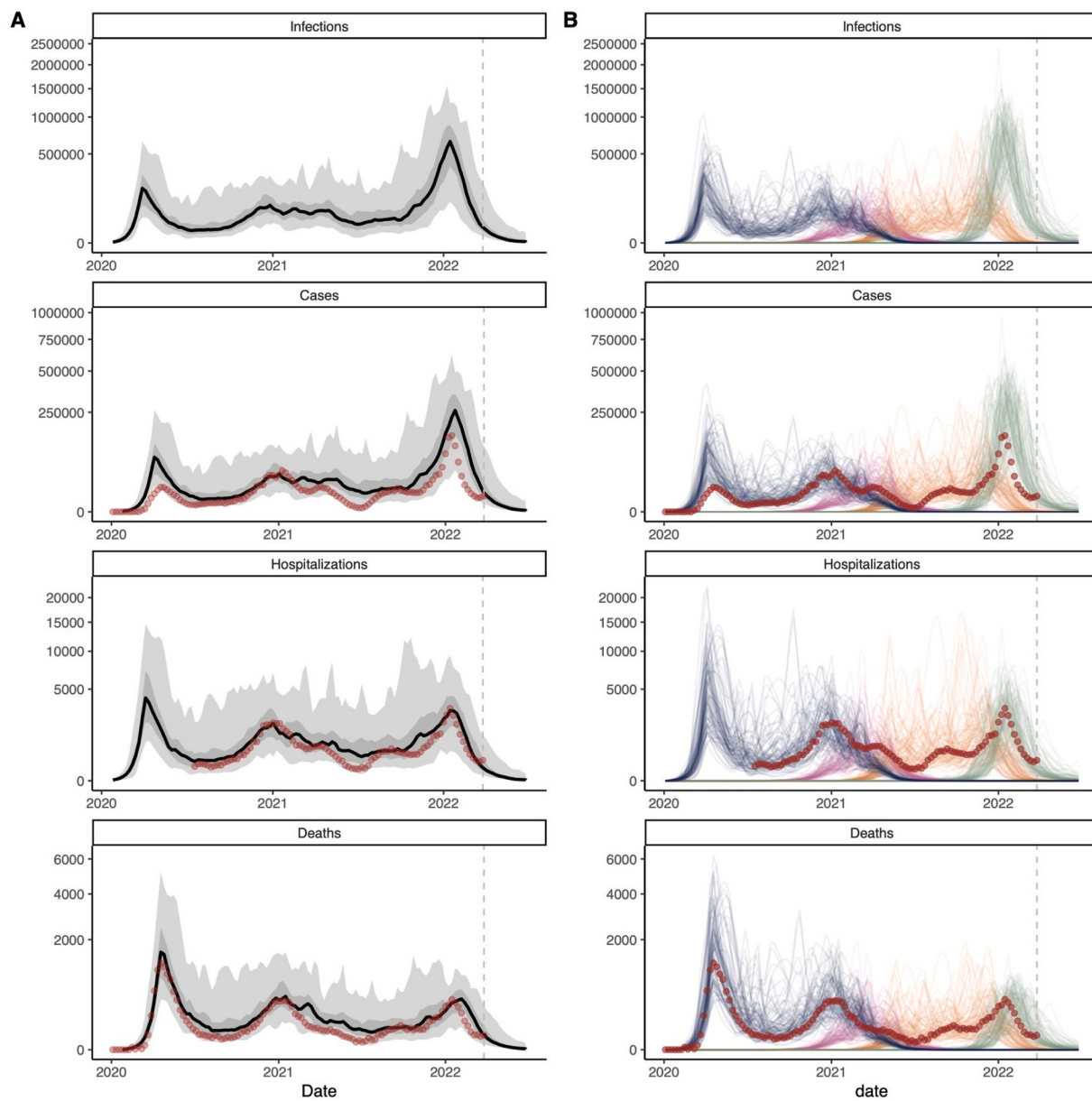


Fig. 7. Model fits to ground truth data for Massachusetts, USA, January 1, 2020 to March 26, 2022. We fit *flepiMoP* to reported incident counts of hospitalizations and deaths for the full US; here we show the results for Massachusetts. In post-production, we produce both (A) weekly quantiles (B) weekly trajectories of simulations. Here we see both the overall fit (A) and the (B) variant-specific trajectories match well with ground truth data (in red) (trajectories: blue = wild type, purple = Alpha variant, orange = Delta variant, green = Omicron variant). The dashed line is the end of the fitting period of these simulations.

demonstrated in our modeling of other pathogens, such as seasonal influenza ([Flu Scenario Modeling Hub, 2022](#)). The workflow described in this paper, leveraging *flepiMoP*'s ability to resume its calibration chain has enabled us to effectively track the evolving course of the pandemic.

Nevertheless, while the framework has shown remarkable flexibility to meet ever-changing demands, there are still areas that require further development and improvement. Despite its empirical performance, the lack of clear information on the theoretical convergence of our inference engine is an important aspect that needs to be addressed. For this, we are looking into the recent development of diagnosis tools for parallel MCMC ([Margossian et al., 2022](#)). Moreover, we plan to build an abstraction layer between the parameter structure of *flepiMoP* and standard statistical inference libraries in Python. This would allow a user to choose between different inference algorithms depending on the desired properties of their use case. Additionally, with the constrained time during the pandemic, we have not fully explored or refined each

component or assumption in the framework. We are actively working to improve these areas. For example, we recently simplified the configuration file and developed a command line interface that greatly streamlines the access to each of the modules within *flepiMoP*.

Another major focus of *flepiMoP* development is to improve accessibility for potential users, beyond the typical walls of scientific research. The demonstrated use of *flepiMoP* in different disease applications and at different spatial scales has proven its potential. In efforts to improve accessibility we have simplified the installation process by reducing *flepiMoP* dependencies and provided documentation and examples for its installation and use on all major platforms. We have also switched internal discussions to public issues on GitHub to include users and dialogue from other users. More broadly, we are continuing to simplify the configuration file syntax and keep the provided documentation up to date.

flepiMoP has proven its value in providing rapid development and

application of disease-appropriate mathematical models and projections for infectious diseases. Its maturity and adaptability make it a valuable tool for researchers and policymakers alike. While improvements are still needed, we are confident that the framework's current capabilities and its open-source nature will contribute to the continued advancement of infectious disease modeling for a wide range of pathogens and demographic contexts.

Data

flepiMoP is an open-source software governed by GPL v3.0 license. It can be found at <https://github.com/HopkinsIDD/flepiMoP/>. Documentation and additional information can be found at flepiMoP.org.

CRediT authorship contribution statement

Joseph Chadi Lemaitre: Conceptualization, Data curation, Formal analysis, Investigation, Methodology, Software, Validation, Visualization, Writing – original draft, Writing – review & editing. **Clifton McKee:** Data curation, Formal analysis, Investigation, Validation, Writing – review & editing. **Elizabeth C Lee:** Formal analysis, Methodology, Software, Validation, Conceptualization, Writing – review & editing. **Joshua Kaminsky:** Formal analysis, Methodology, Software, Validation. **Sara L Loo:** Conceptualization, Data curation, Formal analysis, Investigation, Methodology, Software, Validation, Visualization, Writing – original draft, Writing – review & editing. **Erica Carcelen:** Conceptualization. **Koji Sato:** Software. **Sung-mok Jung:** Data curation, Formal analysis, Investigation, Validation, Writing – review & editing. **Claire Smith:** Data curation, Formal analysis, Investigation, Validation, Writing – review & editing. **Shaun Truelove:** Data curation, Formal analysis, Funding acquisition, Investigation, Project administration, Software, Supervision, Validation, Writing – review & editing. **Justin Lessler:** Conceptualization, Funding acquisition, Methodology, Software, Supervision, Writing – review & editing. **Alison Hill:** Data curation, Formal analysis, Investigation, Methodology, Software, Validation, Visualization, Writing – review & editing.

Declaration of Competing Interest

The authors declare that they have no known competing financial interests or personal relationships that could have appeared to influence the work reported in this paper.

Acknowledgments

We acknowledge the contributions to the original development of the COVID Scenario Pipeline, which evolved into *flepiMoP*. These include contributions by Kyra H. Grantz, Hannah R. Meredith, Stephen A. Lauer, Lindsay T. Keegan, Sam Shah, Josh Wills, Kathryn Kaminsky, and Javier Perez-Saez. Funding for this work was provided by the National Science Foundation (2127976; ST, CPS, JK, ECL, AH), Centers for Disease Control and Prevention (200–2016–91781; ST, CPS, JK, AH, JL, JCL, SLL, CM, EC, KS, S-m.J), US Department of Health and Human Services / Department of Homeland Security (ST, CPS, JK, ECL, AH, JL), California Department of Public Health (ST, CPS, JK, ECL, JL), Johns Hopkins University (ST, CPS, JK, ECL, JL), Amazon Web Services (ST, CPS, JK, ECL, AH, JL, JCL), National Institutes of Health (R01GM140564; JL, 5R01AI102939; JCL), and the Swiss National Science Foundation (200021–172578; JCL).

References

- Asfaw, K., Park, J., King, A.A., Ionides, E.L., 2023. Partially observed Markov processes with spatial structure via the R package *spatPomp*. <https://doi.org/10.48550/arXiv.2101.01157>.
- Bershteyn, A., Gerardin, J., Bridenbecker, D., Lorton, C.W., Bloedow, J., Baker, R.S., Chabot-Couture, G., Chen, Y., Fischle, T., Frey, K., Gauld, J.S., Hu, H., Izzo, A.S., Klein, D.J., Lukacevic, D., McCarthy, K.A., Miller, J.C., Ouedraogo, A.L., Perkins, T.A., Steinkraus, J., ten Bosch, Q.A., Ting, H.-F., Titova, S., Wagner, B.G., Welkhoff, P.A., Wenger, E.A., Wiswell, C.N., for the Institute for Disease Modeling, 2018. Implementation and applications of EMOD, an individual-based multi-disease modeling platform. *fty059 Pathog. Dis.* 76. <https://doi.org/10.1093/femspd/fty059>.
- Borcherding, R.K., Healy, J.M., Cadwell, B.L., Johansson, M.A., Slayton, R.B., Wallace, M., Biggerstaff, M., 2023. Public health impact of the U.S. Scenario Modeling Hub. *Epidemics* 44, 100705. <https://doi.org/10.1016/j.epidem.2023.100705>.
- Bouchnita, A., Bi, K., Fox, S., Meyers, L.A., 2024. Projecting Omicron scenarios in the US while tracking population-level immunity. *Epidemics*.
- Broeck, W.V. den, Gioannini, C., Gonçalves, B., Quaggiotto, M., Colizza, V., Vespuignani, A., 2011. The GLEaMviz computational tool, a publicly available software to explore realistic epidemic spreading scenarios at the global scale. *BMC Infect. Dis.* 11, 37. <https://doi.org/10.1186/1471-2334-11-37>.
- CDC, 2023. FluSight: Flu Forecasting [WWW Document]. Cent. Dis. Control Prev. URL (<https://www.cdc.gov/flu/weekly/fluSight/index.html>) (Accessed 20 August 2023).
- Champredon, D., Dushoff, J., Earn, D.J.D., 2018. Equivalence of the Erlang-Distributed SEIR Epidemic Model and the Renewal Equation. *SIAM J. Appl. Math.* 78, 3258–3278. <https://doi.org/10.1137/18M1186411>.
- Chen, J., Bhattacharya, P., Hoops, S., Machi, D., Adiga, A., Henning Mortveit, Srinivasan Venkatraman, Madhav Marathe, 2024. Role of Heterogeneity: National Scale Data-Driven Agent-Based Modeling for the US COVID-19 Scenario Modeling Hub. *Epidemics*.
- Chinazzi, M., Davis, J.T., Pastore y Piontti, A., Mu, K., Gozzi, N., Marco Ajelli, Nicola Perra, Alessandro Vespuignani, 2024. A Multiscale modeling framework for Scenario Modeling: Characterizing the Heterogeneity of the COVID-19 Epidemic in the US. *Epidemics*.
- COVID Analysis and Mapping of Policies, n.d.
- COVID-19 Forecast Hub [WWW Document], 2020. URL (<https://covid19forecasthub.org/>) (Accessed 18 August 2023).
- Cox, D.R., 2017. The Theory of Stochastic Processes. Routledge, Boca Raton. <https://doi.org/10.1201/9780203719152>.
- Cramer, E.Y., Huang, Y., Wang, Y., Ray, E.L., Cornell, M., Bracher, J., Brennen, A., Rivadeneira, A.J.C., Gerding, A., House, K., Jayawardena, D., Kanji, A.H., Khandelwal, A., Le, K., Mody, Vidhi, Mody, Vrushti, Niemi, J., Stark, A., Shah, A., Wattanchit, N., Zorn, M.W., Reich, N.G., 2022a. The United States COVID-19 Forecast Hub dataset. *Sci. Data* 9, 462. <https://doi.org/10.1038/s41597-022-01517-w>.
- Cramer, E.Y., Ray, E.L., Lopez, V.K., Bracher, J., Brennen, A., Castro Rivadeneira, A.J., Gerding, A., Gneiting, T., House, K.H., Huang, Yuxin, Jayawardena, D., Kanji, A.H., Khandelwal, A., Le, K., Mühlmann, A., Niemi, J., Shah, A., Stark, A., Wang, Yijin, Wattanchit, N., Zorn, M.W., Gu, Y., Jain, S., Bannur, N., Deva, A., Kulkarni, M., Merugu, S., Raval, A., Shingi, S., Tiwari, A., White, J., Abernethy, N.F., Woody, S., Dahan, M., Fox, S., Gaither, K., Lachmann, M., Meyers, L.A., Scott, J.G., Tec, M., Srivastava, A., George, G.E., Cegan, J.C., Dettwiller, I.D., England, W.P., Farthing, M.W., Hunter, R.H., Lafferty, B., Linkov, I., Mayo, M.L., Parno, M.D., Rowland, M.A., Trump, B.D., Zhang-James, Y., Chen, S., Faraone, S.V., Hess, J., Morley, C.P., Salekin, A., Wang, D., Corsetti, S.M., Baer, T.M., Eisenberg, M.C., Falb, K., Huang, Yitao, Martin, E.T., McCauley, E., Myers, R.L., Schwarz, T., Sheldon, D., Gibson, G.C., Yu, R., Gao, Liyao, Ma, Y., Wu, D., Yan, X., Jin, X., Wang, Y.-X., Chen, Y., Guo, L., Zhao, Y., Gu, Q., Chen, J., Wang, Lingxiao, Xu, P., Zhang, W., Zou, D., Biegel, H., Lega, J., McConnell, S., Nagraj, V.P., Guertin, S.L., Hulme-Lowe, C., Turner, S.D., Shi, Y., Ban, X., Walraven, R., Hong, Q.-J., Kong, S., van de Walle, A., Turtle, J.A., Ben-Nun, M., Riley, S., Riley, P., Koyluoglu, U., DesRoches, D., Forli, P., Hamory, B., Kyriakides, C., Leis, H., Milliken, J., Moloney, M., Morgan, J., Nirgudkar, N., Ozcan, G., Piwonka, N., Ravi, M., Schrader, C., Shakhnovich, E., Siegel, D., Spatz, R., Stiefeling, C., Wilkinson, B., Wong, A., Cavany, S., España, G., Moore, S., Oidtmann, R., Perkins, A., Kraus, D., Kraus, A., Gao, Z., Bian, J., Cao, W., Lavista Ferres, J., Li, C., Liu, T.-Y., Xie, X., Zhang, S., Zheng, S., Vespuignani, A., Chinazzi, M., Davis, J.T., Mu, K., Pastore y Piontti, A., Xiong, X., Zheng, A., Baek, J., Farias, V., Georgescu, A., Levi, R., Sinha, D., Wilde, L., Perakis, G., Bennouma, M.A., Nze-Ndong, D., Singhvi, D., Spandidakis, I., Thayaparan, L., Tsiorvas, A., Sarker, A., Jadbabae, A., Shah, D., Della Penna, N., Celi, L.A., Sundar, S., Wolfinger, R., Osthus, D., Castro, L., Fairchild, G., Michaud, I., Karlen, D., Kinsey, M., Mullany, L.C., Rainwater-Lovett, K., Shin, L., Tallaksen, K., Wilson, S., Lee, E.C., Dent, J., Grantz, K.H., Hill, A.L., Kaminsky, J., Kaminsky, K., Keegan, L.T., Lauer, S.A., Lemaitre, J.C., Lessler, J., Meredith, H.R., Perez-Saez, J., Shah, S., Smith, C.P., Truelove, S.A., Wills, J., Marshall, M., Gardner, L., Nixon, K., Burant, J.C., Wang, Lily, Gao, Lei, Gu, Z., Kim, M., Li, X., Wang, G., Wang, Yueying, Yu, S., Reiner, R.C., Barber, R., Gakidou, E., Hay, S.I., Lim, S., Murray, C., Pigott, D., Gurung, H.L., Baccam, P., Stage, S.A., Suchoski, B.T., Prakash, B.A., Adhikari, B., Cui, J., Rodríguez, A., Tabassum, A., Xie, J., Keskinocak, P., Asplund, J., Baxter, A., Oruc, B.E., Serban, N., Arlik, S.O., Dusenberry, M., Epshteyn, A., Kanal, E., Le, L.T., Li, C.-L., Pfister, T., Sava, D., Sinha, R., Tsai, T., Yoder, N., Yoon, J., Zhang, L., Abbott, S., Bosse, N.I., Funk, S., Hellewell, J., Meakin, S.R., Sherratt, K., Zhou, M., Kalantari, R., Yamana, T. K., Pei, S., Shaman, J., Li, M.L., Bertsimas, D., Skali Lami, O., Soni, S., Tazi Bouardi, H., Ayer, T., Adee, M., Chhatwal, J., Daligic, O.O., Ladd, M.A., Linas, B.P., Mueller, P., Xiao, J., Wang, Yuanjia, Wang, Q., Xie, S., Zeng, D., Green, A., Bien, J., Brooks, L., Hu, A.J., Jahja, M., McDonald, D., Narasimhan, B., Politisch, C., Rajanala, S., Rumack, A., Simon, N., Tibshirani, R.J., Tibshirani, R., Ventura, V., Wasserman, L., O'Dea, E.B., Drake, J.M., Pagano, R., Tran, Q.T., Ho, L.S.T., Huynh, H., Walker, J.W., Slayton, R.B., Johansson, M.A., Biggerstaff, M., Reich, N.G., 2022b. Evaluation of individual and ensemble probabilistic forecasts of COVID-19 mortality in the United States. *Proc. Natl. Acad. Sci. USA* 119, e2113561119. <https://doi.org/10.1073/pnas.2113561119>.

- Davies, N.G., Abbott, S., Barnard, R.C., Jarvis, C.I., Kucharski, A.J., Munday, J.D., Pearson, C.A.B., Russell, T.W., Tully, D.C., Washburne, A.D., Wenseleers, T., Gimma, A., Waites, W., Wong, K.L.M., van Zandvoort, K., Silverman, J.D., CMMID COVID-19 Working Group, COVID-19 Genomics UK (COG-UK) Consortium, Diaz-Ordaz, K., Keogh, R., Eggo, R.M., Funk, S., Jit, M., Atkins, K.E., Edmunds, W.J., 2021. Estimated transmissibility and impact of SARS-CoV-2 lineage B.1.1.7 in England. *Science* 372, eabg3055. <https://doi.org/10.1126/science.abg3055>.
- COVID-19 Scenario Modeling Hub [WWW Document], 2020. URL (<https://covid19scenariomodelinghub.org/>) (Accessed 18 August 2023).
- Flu Scenario Modeling Hub [WWW Document], 2022. URL (<https://fluscenariomodelinghub.org/>) (Accessed 20 August 2023).
- Galmiche, S., Cortier, T., Charnet, T., Schaeffer, L., Chény, O., Platen, C., von, Lévy, A., Martin, S., Omar, F., David, C., Mailles, A., Carrat, F., Cauchemez, S., Fontanet, A., 2023. SARS-CoV-2 incubation period across variants of concern, individual factors, and circumstances of infection in France: a case series analysis from the ComCor study. *Lancet Microbe* 4, e409–e417. [https://doi.org/10.1016/S2666-5247\(23\)00005-8](https://doi.org/10.1016/S2666-5247(23)00005-8).
- Goldberg, Y., Mandel, M., Bar-On, Y.M., Bodenheimer, O., Freedman, L.S., Ash, N., Alroy-Preis, S., Huppert, A., Milo, R., 2022. Protection and Waning of Natural and Hybrid Immunity to SARS-CoV-2. *N. Engl. J. Med.* 386, 2201–2212. <https://doi.org/10.1056/NEJMoa2118946>.
- Hodcroft, E., 2021. CoVariants: SARS-CoV-2 Mutations and Variants of Interest [WWW Document]. URL (<https://covariants.org/>) (Accessed 18 August 2023).
- Howerton, E., Contamin, L., Mullany, L.C., Qin, M., Reich, N.G., Bents, S., Borchering, R.K., Jung, S., Loo, S.L., Smith, C.P., Levander, J., Kerr, J., Espino, J., Panhuis, W.G., van Hochheiser, H., Galanti, M., Yamana, T., Pei, S., Shaman, J., Rainwater-Lovett, K., Kinsey, M., Tallaksen, K., Wilson, S., Shin, L., Lemaitre, J.C., Kaminsky, J., Hulse, J.D., Lee, E.C., McKee, C., Hill, A., Karlen, D., Chinazzi, M., Davis, J.T., Mu, K., Xiong, X., Piontti, A.P. y, Vesprini, A., Rosenstrom, E.T., Ivy, J.S., Mayorga, M.E., Swann, J.L., España, G., Cavany, S., Moore, S., Perkins, A., Hladish, T., Pillai, A., Toh, K.B., Longini, I., Chen, S., Paul, R., Janies, D., Thill, J.-C., Bouchnita, A., Bi, K., Lachmann, M., Fox, S., Meyers, L.A., Consortium, U.C.-19 M., Srivastava, A., Porebski, P., Venkatramanan, S., Adiga, A., Lewis, B., Klahn, B., Outten, J., Hurt, B., Chen, J., Mortveit, H., Wilson, A., Marathe, M., Hoops, S., Bhattacharya, P., Machi, D., Cadwell, B.L., Healy, J.M., Slayton, R.B., Johansson, M.A., Biggerstaff, M., Truelove, S., Runge, M.C., Shea, K., Viboud, C., Lessler, J., 2023. Informing pandemic response in the face of uncertainty: An evaluation of the U.S. COVID-19 Scenario Modeling Hub. <https://doi.org/10.1101/2023.06.28.23291998>.
- Hurtado, P.J., Kirosingh, A.S., 2019. Generalizations of the “Linear Chain Trick”: Incorporating more flexible dwell time distributions into mean field ODE models. *J. Math. Biol.* 79, 1831–1883. <https://doi.org/10.1007/s00285-019-01412-w>.
- Johns Hopkins University, Bloomberg Center for Government Excellence, 2020. Johns Hopkins Coronavirus Resource Center Dataset.
- Kerr, C.C., Stuart, R.M., Mistry, D., Abeyseuriya, R.G., Rosenfeld, K., Hart, G.R., Núñez, R.C., Cohen, J.A., Selvaraj, P., Hagedorn, B., George, L., Jastrzębski, M., Izzo, A.S., Fowler, G., Palmer, A., Delport, D., Scott, N., Kelly, S.L., Bennette, C.S., Wagner, B.G., Chang, S.T., Oron, A.P., Wenger, E.A., Panovska-Griffiths, J., Famulari, M., Klein, D.J., 2021. Covasim: an agent-based model of COVID-19 dynamics and interventions. *PLoS Comput. Biol.* 17, e1009149 <https://doi.org/10.1371/journal.pcbi.1009149>.
- King, A.A., Nguyen, D., Ionides, E.L., 2015. Statistical Inference for Partially Observed Markov Processes via the R Package pomp. *ArXiv150900503 Stat.*
- Lemaitre, J.C., Grantz, K.H., Kaminsky, J., Meredith, H.R., Truelove, S.A., Lauer, S.A., Keegan, L.T., Shah, S., Wills, J., Kaminsky, K., Perez-Saez, J., Lessler, J., Lee, E.C., 2021. A scenario modeling pipeline for COVID-19 emergency planning. *Sci. Rep.* 11, 7534. <https://doi.org/10.1038/s41598-021-86811-0>.
- Lloyd, A.L., 2001. Realistic Distributions of Infectious Periods in Epidemic Models: Changing Patterns of Persistence and Dynamics. *Theor. Popul. Biol.* 60, 59–71. <https://doi.org/10.1006/tpbi.2001.1525>.
- Loo, S.L., Howerton, E., Contamin, L., Smith, C.P., Borchering, R.K., Mullany, L.C., Bents, S., Carcelen, E., Jung, S., Bogich, T., van Panhuis, W.G., Kerr, J., Espino, J., Yan, K., Hochheiser, H., Runge, M.C., Shea, K., Lessler, J., Viboud, C., Truelove, S., 2024. The US COVID-19 and Influenza Scenario Modeling Hubs: Delivering long-term projections to guide policy. *Epidemics* 46, 100738. <https://doi.org/10.1016/j.epidem.2023.100738>.
- Lumley, S.F., O'Donnell, D., Stoesser, N.E., Matthews, P.C., Howarth, A., Hatch, S.B., Marsden, B.D., Cox, S., James, T., Warren, F., Peck, L.J., Ritter, T.G., de Toledo, Z., Warren, L., Axten, D., Cornall, R.J., Jones, E.Y., Stuart, D.I., Scratton, G., Ebner, D., Hoosdally, S., Chand, M., Crook, D.W., O'Donnell, A.-M., Conlon, C.P., Pouwels, K.B., Walker, A.S., Petro, T.E.A., Hopkins, S., Walker, T.M., Jeffery, K., Eyre, D.W., 2021. Antibody status and incidence of SARS-CoV-2 infection in health care workers. *N. Engl. J. Med.* 384, 533–540. <https://doi.org/10.1056/NEJMoa2034545>.
- Margossian, C.C., Hoffman, M.D., Sountsov, P., Riou-Durand, L., Vehtari, A., Gelman, A., 2022. Nested \$\\hat{\\lambda}\$ and RS: Assessing the convergence of Markov chain Monte Carlo when running many short chains. <https://doi.org/10.48550/arXiv.2110.13017>.
- Mniszewski, S.M., Del Valle, S.Y., Stroud, P.D., Riese, J.M., Sydoriak, S.J., 2008. EpiSimS simulation of a multi-component strategy for pandemic influenza, in: Proceedings of the 2008 Spring Simulation Multiconference, SpringSim '08. Society for Computer Simulation International, San Diego, CA, USA, pp. 556–563.
- Moore, S., Cavany, S., Perkins, T.A., Guido Felipe, Espana, C., 2024. Projecting the future impact of emerging SARS-CoV-2 variants under uncertainty: modeling the initial Omicron outbreak. *Epidemics*.
- National Center for Health Statistics Mortality Surveillance System, n.d. FluView: Pneumonia and Influenza Mortality Surveillance [WWW Document]. URL (<https://gis.cdc.gov/grasp/fluview/mortality.html>) (accessed 8.18.23).
- Pillai, A.N., Toh, K.B., Perdomo, D., Bhargava, S., Stoltzfus, A., Ira M.Longini, Jr, Carl A.B. Pearson, Thomas J. Hladish, 2024. Agent-based modeling of the COVID-19 pandemic in Florida.
- Porebski, P., Venkatramanan, S., Adiga, A., Klahn, B., Hurt, B., Mandy L. Wilson, Jiangzhuo Chen, Anil Vulikanti, Madhav Marathe, Bryan Lewis, 2024. Data-driven mechanistic framework with stratified immunity and effective transmissibility for COVID-19 scenario projections. *Epidemics*.
- New York Times, 2020. See. Reopening Plans and Mask Mandates for All 50 States. Times.
- Pulliam, J.R.C., van Schalkwyk, C., Govender, N., von Gottberg, A., Cohen, C., Groome, M.J., Dushoff, J., Mlisana, K., Moultrie, H., 2022. Increased risk of SARS-CoV-2 reinfection associated with emergence of Omicron in South Africa. *Science* 376, eabn4947. <https://doi.org/10.1126/science.abn4947>.
- Reich, N.G., McGowan, C.J., Yamana, T.K., Tushar, A., Ray, E.L., Osthus, D., Kandula, S., Brooks, L.C., Crawford-Crudell, W., Gibson, G.C., Moore, E., Silva, R., Biggerstaff, M., Johansson, M.A., Rosenfeld, R., Shaman, J., 2019. Accuracy of real-time multi-model ensemble forecasts for seasonal influenza in the U.S. *PLoS Comput. Biol.* 15, e1007486. <https://doi.org/10.1371/journal.pcbi.1007486>.
- Rosenstrom, E.T., Ivy, J.S., Mayorga, M.E., Swann, J.L., 2024. COVISim: a stochastic agent-based COVID-19 SIMulation Model for North Carolina. *Epidemics*.
- Shaman, J., Pitzer, V.E., Viboud, C., Grenfell, B.T., Lipsitch, M., 2010. Absolute humidity and the seasonal onset of influenza in the continental United States. *PLoS Biol.* 8, e1000316 <https://doi.org/10.1371/journal.pbio.1000316>.
- Srivastava, A., 2023. The variations of SIRAlpha model for COVID-19 forecasting and scenario projections. *Epidemics* 45, 100729. <https://doi.org/10.1016/j.epidem.2023.100729>.
- Srivastava, A., Xu, T., Prasanna, V.K., 2020. Fast and Accurate Forecasting of COVID-19 Deaths Using the SIRAlpha Model. <https://doi.org/10.48550/arXiv.2007.05180>.
- Taylor, C.A., 2021. Severity of Disease Among Adults Hospitalized with Laboratory-Confirmed COVID-19 Before and During the Period of SARS-CoV-2 B.1.617.2 (Delta) Predominance — COVID-NET, 14 States, January–August 2021. *MMWR Morb. Mortal. Wkly. Rep.* 70 <https://doi.org/10.15585/mmwr.mm7043e1>.
- US Census Bureau, U.C., 2015. 2011–2015 5-Year ACS Commuting Flows [WWW Document]. URL (<https://www.census.gov/data/tables/2015/demo.metro-micro-commuting-flows-2015.html>) (Accessed 5 May 2023).
- U.S. Department of Health & Human Services, 2020. COVID-19 Reported Patient Impact and Hospital Capacity by State Timeseries. [WWW Document]. URL (<https://healthdata.gov/Hospital/COVID-19-Reported-Patient-Impact-and-Hospital-Capa/g62h-syeh>) (Accessed 18 August 2023).
- Wearing, H.J., Rohani, P., Keeling, M.J., 2005. Appropriate Models for the Management of Infectious Diseases. *PLoS Med.* 2, e174 <https://doi.org/10.1371/journal.pmed.0020174>.